

*Research article*

## **Methodology for the characterization of the humidity behavior inside CPV modules**

**Carmine Cancro, Gabriele Ciniglio, Luigi Mongibello \*, and Antonino Pontecorvo**

ENEA—Italian National Agency for New Technologies, Energy and Sustainable Economic Development, Portici Research Center, P.le E.Fermi, 1 – 80055 Portici (NA), Italy

\* **Correspondence:** Email: [luigi.mongibello@enea.it](mailto:luigi.mongibello@enea.it); Tel: +39-081-7723584;  
Fax: +39-081-7723344.

**Abstract:** In this study the characterization of the humidity behavior inside concentrating photovoltaic (CPV) modules is addressed. To this purpose, several experimental tests have been carried out by using two different CPV modules and three different breathers, collecting in each analyzed case the evolution of temperature, relative and specific humidity of the air volume contained inside the module for many days. Results indicates that, for each of the CPV modules analyzed, it is possible to construct a characteristic curve in the temperature-specific humidity psychrometric chart, that can be used for estimating the specific humidity of the air inside the CPV module as a function of the internal air temperature. The characteristic curve can be also used to estimate the saturation temperature of the air inside the CPV module, and consequently to detect the eventuality of moisture condensation during cloudy days or night-time, namely when the temperature of the air inside the module is low and reaches the external ambient one. This methodology can be used in CPV modules design for the choice of the breather and of the construction materials, in order to obtain a saturation temperature as low as possible.

**Keywords:** CPV module; relative and specific humidity; experimental tests, fitting curve; extrapolation of saturation temperature

---

### **1. Introduction**

Moisture condensation into CPV modules constitutes one of the most relevant causes which may limit their performance and lifetime. Indeed, the possibility of CPV systems to penetrate the PV

market also depends on these factors. Thus, in order to prevent that minute water droplets can degrade the CPV performance and damage electronic devices, it is essential that the specific humidity inside the package in which they are contained does not reach saturation values.

A CPV module is normally constituted by several PV receivers physically placed in the focal points of the concentration system. A rigid housing is normally used to fix concentrators and cells in the right positions, and to protect the module sensitive components, as electrical contacts, cells, diodes from the external environmental agents. For this reason a CPV module is mostly realized as a box, typically having a transparent window allowing the light entrance, and containing the concentration system (that in the case of use of refractive lenses technology can be integrated with the transparent window), and the PV receivers electrically connected to each other.

During sunny days, the temperature of the air volume contained inside a CPV module increases because of the heat absorbed by the housing walls, and because of the heat dissipated internally by the cells. In case of completely sealed module, the temperature increase would determine a relevant pressure increase, which could cause mechanical damages to the housing structure. Thus, in order to keep the air pressure inside CPV modules constant, these are normally provided with a duct, called breather, that allows air exit and entrance during heating and cooling times, respectively. The breather is usually equipped with a filter in order to avoid the entrance of dust or insects inside the module housing. During the thermal cycles it can be observed that the relative and specific humidity factors of the air volume inside CPV modules change continuously, and this variation of the air water vapor content is essentially due to two reasons. Namely, the water vapor exchange with the external environment occurs both through the breather by diffusion, and through the water absorption/desorption of the materials constituting the CPV modules which are characterized by a non-negligible water absorptivity, with particular reference to the sealing substances [1–9]. These phenomena, in particular weather conditions, can cause the moisture condensation inside the CPV modules, that in turn can involve several technical problems.

Figure 1 shows condensed moisture accumulated on the inner side of the Silicon on Glass Fresnel lenses of a CPV module installed at ENEA Portici RC. In this case the condensed moisture determines a diffusion of the solar radiation, and as a consequence an inefficiency of the optical concentrator system, that in turn determines a strong decrease of the electric energy produced by the module. Moreover, the presence of small water droplets on the lenses or mirrors surface can accelerate the degradation processes of these components. For refractive optics, humidity freeze tests revealed that the water presence acts as a sort of catalyzer for chemical reactions producing a local consumption of glass or lenses substrate [10]. This determines the formation of small cavities and grooves on the optic surface, and consequently a strong increase of the scattering losses. As regards reflective optics, it has to be pointed out that, since they are mostly realized by means of metallic layers deposited on glass or plastic substrates, the presence of water accelerates their oxidation processes [11]. Moreover, water promotes the mechanical adhesion of fine dust and particulate on both the refractive and the reflective surfaces, determining the decrease of their optical performances.

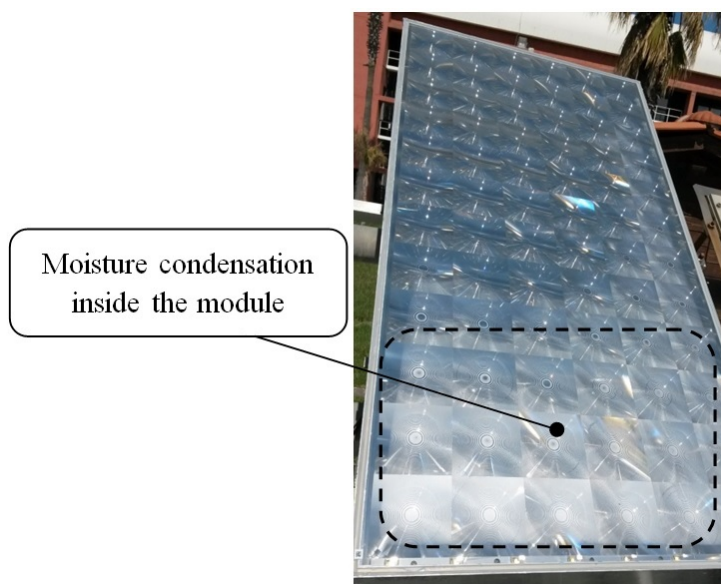


**Figure 1. CPV module with condensed moisture deposited on the lower side of the inner surface of the lenses parquet.**

Relatively to electronics, the presence of condensed moisture inside the module can cause corrosion of cell interconnects and solder joints, with a consequent increase in the series resistance. Water droplets on the receiver substrate can determine electrical contact between positive and negative electrodes, then PV cells short circuit can occur. Furthermore, condensed moisture causes the decrease of the module insulating resistance, that in particular conditions can cause the plant shutdown.

The present work deals with the characterization of humidity behavior inside CPV modules. To this purpose, several experimental tests have been carried out by using two different CPV modules and three different breathers, collecting in each analyzed case the evolution of temperature, relative and specific humidity of the air volume contained inside the module for many days. In the following, the details about the experimental tests are reported in section 2, while the experimental results and their analysis are reported in section 3. The conclusions are reported in section 4.

## **2. Materials and Method**

The experimental tests have been performed using two different CPV modules. The first one, developed by ENEA and other Italian partners within the PhoCUS Project (Photovoltaic Concentrator to Utility Scale) in the early 2000s, is mainly realized in plastic material. The second one has been recently developed by the Italian Company BECAR together with other Industrial and academic partners within the European ECOSOLE Project (Elevated Concentration photovoltaic solar energy generator and fully automated machinery for high throughput manufacturing and testing). It is realized using aluminum for the housing and glass for the front window. For each of the above modules, three different breathers have been tested. The first home-made one consists of a labyrinthine filter with a sponge inside, the second one consists of the first one without the sponge, while the third commercial one consists of a metallic foam filter.

## 2.1. Modules

Figure 2 shows a picture and a schematic of the PhoCUS CPV module [12]. Its housing is made of a plastic thermo-forming material to assure the desired mechanical resistance and a good protection against the environmental agents. The PV receivers are electrically connected and placed on the bottom of the housing. The cells are individually placed on an aluminum heat sink fixed on the housing bottom. The front optical window consists of a lenses parquet, based on prismatic/hybrid PMMA (polymethylmethacrylate) lenses, while secondary optical element (SOE) consists of a plastic pyramid having the inner surface covered by a reflective metallic sheet. The electrical cabling is realized with copper strips fixed on the plastic housing. The PhoCUS CPV module overall dimensions are  $1.0\text{ m} \times 0.68\text{ m} \times 0.25\text{ m}$ , and its weight is approximately 30 kg.



**Figure 2. PhoCUS CPV module schematic view and picture.**

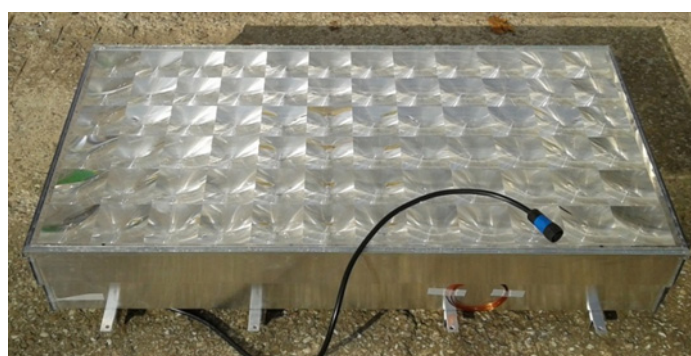


**Figure 3. ECOSOLE CPV module.**

The ECOSOLE module is realized with a Silicon on Glass Fresnel lenses parquet glued using a silicone bead to the upper frame of a metallic enclosure, which hosts the solar receivers on its internal bottom layer. The enclosure consists of three parts, namely an U-shaped aluminum sheet and two lateral panels made of plastic. The 72 HCPV receivers, realized with III-V PV cells, coupled

with secondary quartz elements (SOE) acting as homogenizers and secondary concentrators, are attached to the bottom aluminum sheet. The module is shown in Figure 3. Its dimensions are 1142 mm × 590 mm × 200 mm.

## 2.2. Breathers

Figure 4 shows the home-made breather. It consists of a labyrinthine filter that has to be mounted on one of the module wall so that its long side is vertically oriented and the aperture faces downward when the system is in the parking position (during night-time). During the CPV modules cooling phase, when air enters the module housing, the labyrinthine duct decelerates the air flow so that the dust is deposited on it. During night-time, thanks to the gravity, the dust slips out of the filter. A second trap for smaller dust particles is realized by two coaxial cylinders at the module entrance. Its main dimensions are 100 mm × 45mm × 20 mm. As already reported, this component has been tested both with and without a sponge inserted in the labyrinthine duct.

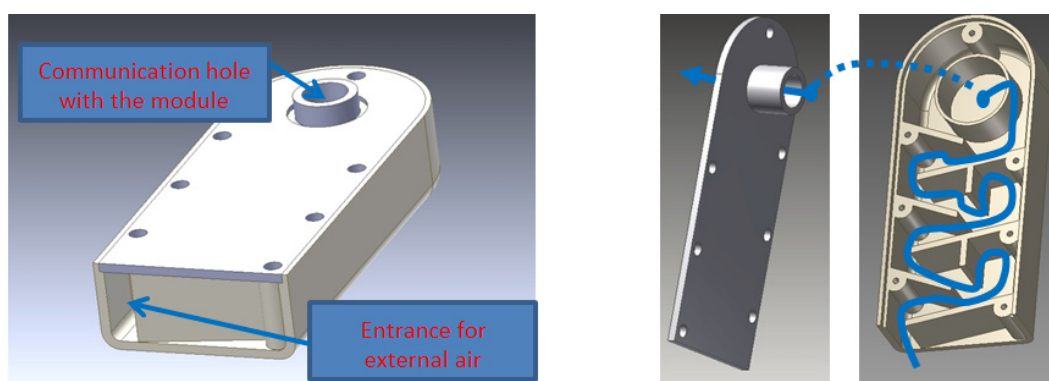


**Figure 4. Home-made breather.**



**Figure 5. Commercial breather.**

Figure 5 shows a picture of the commercial breather. It consists of a metallic-foam filter realized by a steel cylindrical casing with an end consisting of a smaller diameter threaded shank used to fix the component to the module housing. The cylindrical casing is filled with a sintered brass element acting as a filter to protect an hydrophobic membrane paced at its end. The openings are represented

by the internal edge of the shank, and by an annulus opening placed at the lower part of the larger cylinder .

### 2.3. Tests set-up

The outdoor experimental tests have been performed at the ENEA Portici Research Center. Figure 6 shows the modules as they have been tested for the present study. As it can be noticed, the experimental tests have been done with the two modules fixed on the ground (without tracking), with the normal to the front surface vertically oriented, and with no electrical loads. It can be also noticed that the ECOSOLE module (the one on the right) has been tested with a glass in place of the lenses parquet, and with a black painted metallic sheet inside in order to obtain high values for the internal air temperature.



**Figure 6. Tested modules.**

Two Galltec+Mela thermo-hygrometers type TFG80J have been used for the measurement of the relative humidity and temperature of the air inside the modules. The relative humidity measuring range of the above instruments is 0–100%, with an accuracy  $\pm 2.5\%$  for values of the relative humidity higher than 40%, while the temperature measuring range is  $-30\text{ }^{\circ}\text{C}$ – $+80\text{ }^{\circ}\text{C}$ , with an accuracy  $\pm 0.5\text{ }^{\circ}\text{C}$ . Each thermo-hygrometer was placed in a box, connected to the module housing having a degree of water protection IP66. Data relative to the external environment have been measured by means of a weather station installed at the ENEA Portici RC.

Three experimental campaigns have been conducted, each lasting 22 days. In the first one, starting from March 13, 2015, both modules were equipped with the home-made breather with the sponge inside. In the second one from April 9, 2015, both modules included the home-made breather without the sponge, while in the last one from May 6, 2015 the commercial breather was used for both modules. The experimental data relative to the air inside the modules have been recorded with a sampling time of 60 seconds by means of a Madgetch QuadProcess data logger.

### 3. Results and Discussion

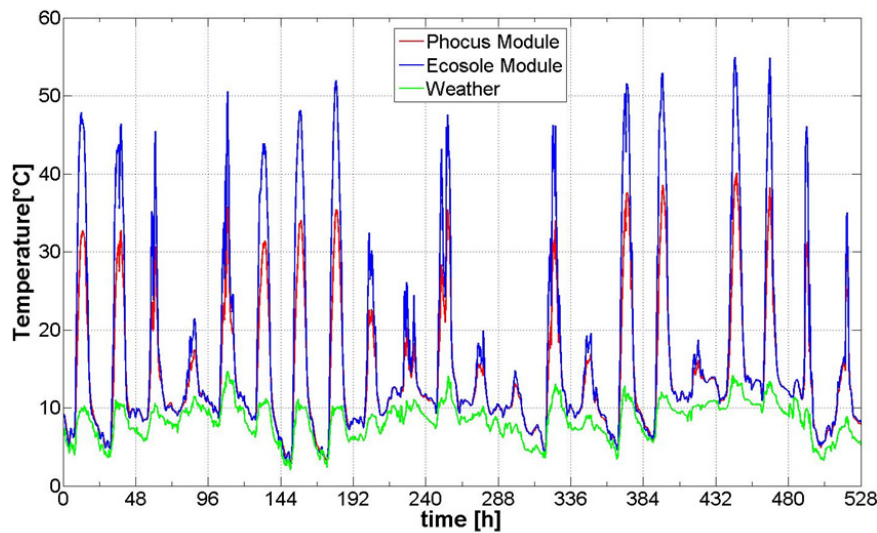
Figures 7, 8 and 9 show the temporal evolution of modules internal air and ambient air temperature, specific humidity and relative humidity, respectively, measured during the first test, namely the one with the home-made breather including a sponge mounted on both modules. The values of specific humidity has been evaluated from the measured values of relative humidity and temperatures by means of a Mollier chart. As concerns the modules internal air behavior, it can be noticed that, as it was to be expected, for both modules the specific humidity increases with the increase in temperature, while the relative humidity shows an opposite trend. Indeed, the relative humidity increases as the temperature decreases, i.e. during night-time or cloudy periods. It can be also noticed that the ECOSOLE module presents temperature peaks much higher than the PhoCUS ones, and this is essentially due to the presence of the black metallic sheet inside the ECOSOLE module. As already stated, the variation of the internal air water vapor content, i.e. the specific humidity, is due to the water vapor exchange with the external environment through the breather by diffusion, and to the water absorption/desorption relative to the materials constituting the CPV modules that present a non-negligible water absorptivity, with particular reference to the sealing substances. Among the above two phenomena, it can be stated that the most relevant one is represented by the water absorption/desorption of the modules materials. In fact, in figure 8 it can be noticed that during sunny days, when the internal air temperature reaches values much higher than the ambient one, the water vapor concentration inside the modules increases and assumes values much higher than the external air one. This is due to the water desorption of the modules materials, that would not happen in case the most relevant water vapor exchange mechanism was the diffusion through the breather, as this mechanism prescribes the water vapor exit from the module when the its concentration in the internal air is higher than the one in the external environment. Equivalently, when the air internal temperature decreases, the specific humidity inside the modules decreases due to the water absorption by the modules materials.

Figure 10 shows the temperature-specific humidity maps of the experimental data relative to the two modules mounting the home-made breather with the sponge. For each module, a fitting curve with the following exponential expression has been derived:

$$y = a \cdot e^{b \cdot x} \quad (1)$$

The values of the coefficients  $a$  and  $b$  have been calculated by using the Matlab exponential fitting function including weights. In particular, the best fitting function has been constructed so that for each module the exponential curve passes through the two points characterized by the minimum and maximum temperature, respectively. Moreover, in each case the fictitious point of coordinates  $(-273 \text{ }^\circ\text{C}, 0 \text{ gram water/kg dry air})$  has been added to the experimental points to prevent fitting curves cramming into the negative specific humidity plane at negative temperature values close to  $0 \text{ }^\circ\text{C}$ . As can be argued, the fitting curve depends on the module characteristics, and also on the characteristic of the external environment. In this case, for the PhoCUS module the coefficients  $a$  and  $b$  are equal to 2.512 and 0.05664, respectively, with the coefficient of determination  $R^2$  equal to 0.9471, while for the ECOSOLE module the coefficients  $a$  and  $b$  are equal to 2.965 and 0.04473, respectively, with a coefficient of determination equal to 0.9061. The two fitting curves are also included in figure 10. By analyzing the fitting curves, it can be noticed that at high temperatures, for

a fixed value of the internal air temperature, the Phocus module presents a higher value of the specific humidity than the ECOSOLE one, and this can be addressed to the higher water desorption in the PhoCUS module due to the plastic housing characterized by a relatively high water absorptivity. On the contrary, at low temperatures the Phocus module presents lower values of the specific humidity than the ECOSOLE one, and this can be also addressed to the higher water absorptivity of the PhoCUS module plastic housing.



**Figure 7. Experimental temperatures.**

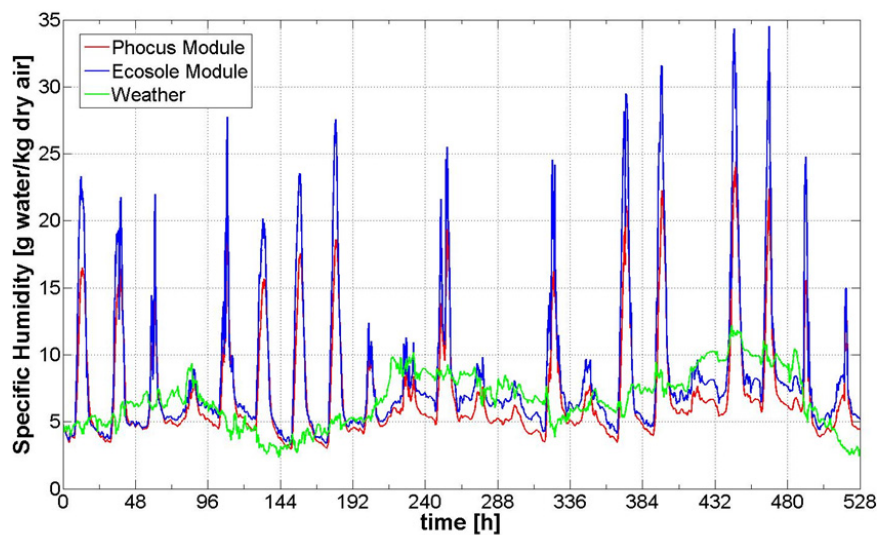


**Figure 8. Experimental specific humidity.**



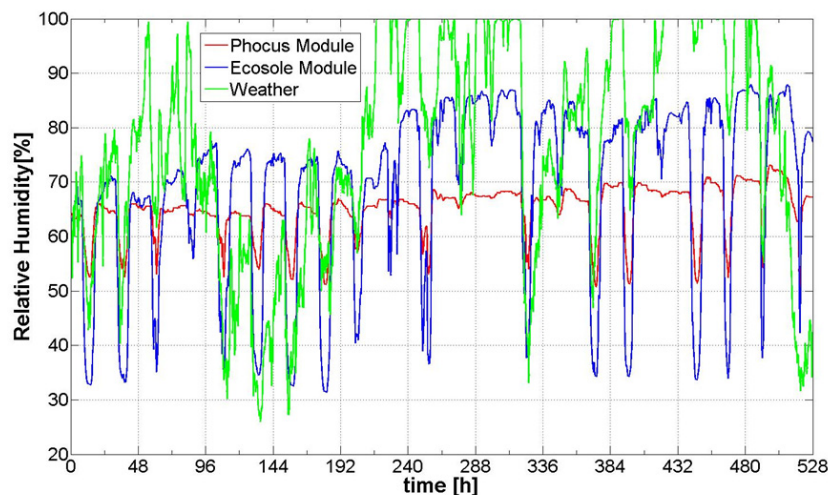


**Figure 9. Experimental relative humidity.**

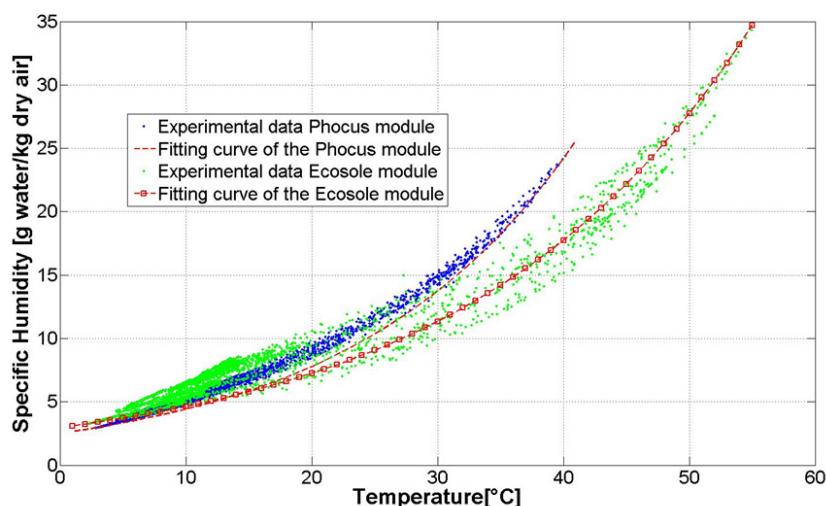


**Figure 10. Maps of experimental data and fitting curves.**

Figures 11 and 12 shows the comparison between the experimental values of the specific humidity and those calculated by means of the fitting curves using the experimental temperatures as input for the Phocus and the ECOSOLE module, respectively. It can be noticed that the fitting curves permit to obtain a good approximation of the specific humidity behavior, especially in proximity of the absolute minimum and maximum temperatures, that are reached after 150 h and 440 h, respectively. Figure 13 shows the fitting curves in the dry bulb temperature-specific humidity psychrometric chart, in which the saturation curve is represented by the continuous red one. By intersecting the fitting curves with the saturation one, it is possible to extrapolate for both modules the value of the saturation temperature, at which water condenses. In the present case, the estimated saturation temperature for the ECOSOLE module is about  $-8.5\text{ }^{\circ}\text{C}$ , while for the PhocUS one it is lower than  $-10\text{ }^{\circ}\text{C}$ .

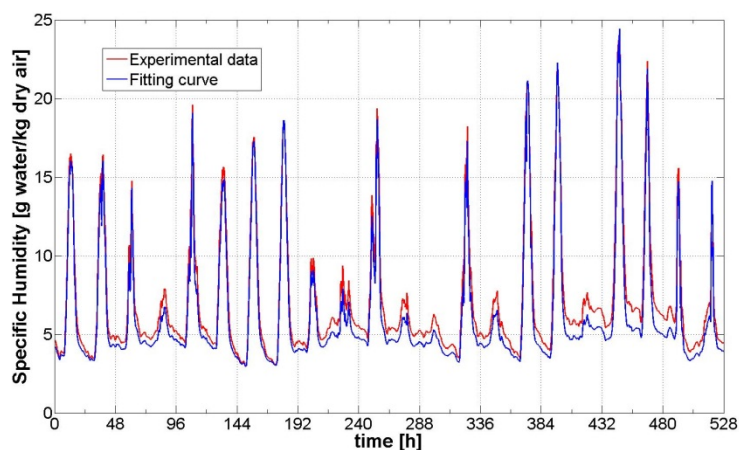


**Figure 11. Comparison between experimental and modeled specific humidity for the PhoCUS module.**

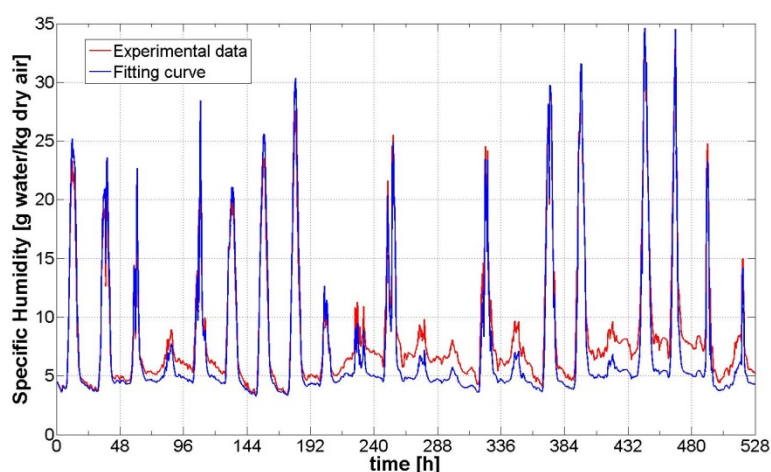


**Figure 12. Comparison between experimental and modeled specific humidity for the ECOSOLE module.**

Finally, tables 1 and 2 report the main data resulting from all the experimental tests of the PhoCUS module and the ECOSOLE one, respectively, and from the application of the fitting algorithm. Considering the values of the coefficient of determination  $R^2$ , in general they are very close to 1, meaning that the fitting curves permit to obtain a good representation of the experimental data. Moreover, it can be noticed that, for each module, the value of  $R^2$  relative to the home-made breather without the sponge and the one relative to the commercial breather are similar, while the one relative to the home-made breather with the sponge is lower than the other two. This result indicates that in general the presence of the sponge leads to a larger range of values of the specific humidity that the air inside the modules can assume. However, it has to be considered that in all analyzed cases the fitting curve has been constructed in order to obtain a very good representation of the experimental data at low temperatures, namely close to the saturation one, where the variance of

experimental data is very low, as can be seen in figure 10. As concerns the values of the saturation temperature, it can be stated that the PhoCUS module presents a better behavior of the internal air humidity, because for all breathers it is characterized by a saturation temperature lower than the one relative to the ECOSOLE module. For the same reason it can be stated that the best breather is the home-made one with the sponge inside.

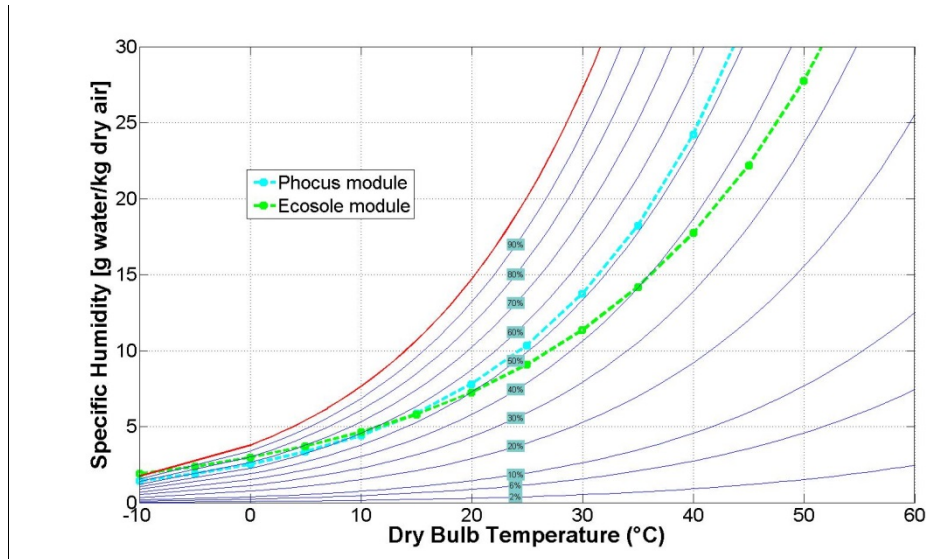


Figure 13. Fitting curves in the dry bulb temperature-specific humidity psychrometric chart.

Table 1. Data for the Phocus module.

	Home-made breather with sponge	Home-made breather without sponge	Commercial breather
$a$	2.512	2.779	2.98
$b$	0.05664	0.05006	0.04865
$R^2$	0.9471	0.9835	0.9934
Saturation temperature	-12 °C	-10 °C	-9 °C

Table 2. Data for the ECOSOLE module.

	Home-made breather with sponge	Home-made breather without sponge	Commercial breather
$a$	2.965	3.345	3.544
$b$	0.04473	0.04162	0.04289
$R^2$	0.9061	0.9789	0.9714
Saturation temperature	-8.5 °C	-6.5 °C	-5.5 °C

## 4. Conclusion

In this work the results of experimental tests aimed at understanding the behavior of the humidity relative to the air contained inside the CPV modules have been shown. Several experimental tests have been carried out by using two different CPV modules and three different breathers, recording in each analyzed case the evolution of temperature, relative and specific humidity of the air volume contained inside the module for many days. From experimental data it has emerged that for each module the correlation between temperature and specific humidity of the internal air can be represented by an exponential characteristic curve in the temperature-specific humidity psychrometric chart, that essentially depends on the module, and in particular on its construction materials. This represents the major result of the present study, and the adopted methodology can be used to construct the characteristic curve for any CPV module in order to estimate the specific humidity of the internal air as a function of the internal air temperature. Furthermore, the present methodology can be used to estimate the saturation temperature of the air inside any CPV module, and consequently to detect the eventuality of moisture condensation during cloudy days or night-time, namely when the temperature of the air inside the module is low and reaches the external ambient one. Finally, this methodology can be used in CPV modules design for the choice of the breather and of the construction materials, in order to obtain a saturation temperature as low as possible.

## Acknowledgments

This project has received funding from the European Union's Seventh Framework Program for research, technological development and demonstration under grant agreement no 295985 (Project acronym: ECOSOLE). This publication reflects the views only of the authors and the European Commission cannot be held responsible for any use which may be made of the information contained therein.

## Conflict of Interest

All authors declare no conflicts of interest in this paper.

## References

1. Hülsmann P, Weiss KA (2015) Simulation of water ingress into PV-modules: IEC-testing versus outdoor exposure. *Sol Energ* 115: 347–353.
2. Hülsmann P, Weiß KA, Köhl M (2012) Temperature-dependent water vapour and oxygen permeation through different polymeric materials used in photovoltaic-modules. *Progress in Photovoltaics: Res Appl* 22: 415–421.
3. Kempe MD (2006) Modeling of rates of moisture ingress into photovoltaic modules. *Sol Energ Mater Sol Cell* 90: 2720–2738.
4. Hülsmann P, Philipp D, Köhl M (2009) Measuring temperature-dependent water vapor and gas permeation through high barrier films. *Rev Sci Instrum* 80: 113901.

5. Hülsmann P, Heck M, Köhl M (2013) Simulation of Water Vapor Ingress into PV-Modules under Different Climatic Conditions. *J Mater* 2013. Available from: <http://dx.doi.org/10.1155/2013/102691>.
6. Vogt A, Peharz G, Jaus J, et al. (2006) Degradation Studies on FLATCON® Modules and Assemblies, 21st European Photovoltaic Solar Energy Conference, Dresden, Germany.
7. Kempe M, Dameron A, Reese M (2013) Evaluation of moisture ingress from the perimeter of photovoltaic modules. *Prog Photovol Res Appl* 22: 1159–1171.
8. Reisner E, Stollwerck G, Peerlings H, et al. (2006) Humidity in a solar module - horror vision or negligible, 21st European Photovoltaic Solar Energy Conference, Dresden, Germany.
9. Kempe MD (2005) Control of Moisture Ingress into Photovoltaic Modules, 31st IEEE Photovoltaics Specialists Conference and Exhibition Lake Buena Vista, Florida.
10. Mikami R, Toya K, Saito K, et al. (2015) CPV module's reliability test results and the degradation by glass dimming, Proceeding of 11th International Conference on Concentrator Photovoltaic Systems-Aix Les Bains.
11. Kennedy CE, Terwilliger K, Jorgensen GJ (2007) Further analysis of accelerated exposure testing of thin-glass mirror matrix, Proceedings of ES2007 Energy Sustainability 2007, Long Beach, California.
12. Fucci R, Cancro C, Graditi G, et al. (2011) ENEA's activities on C-PV technology, Proceeding of International Conference in Clean Electrical Power, Ischia, Italy.
13. Cancro C, Graditi G, Fucci R, et al. (2015) Characterization And Validation Tests On Ecosole C-Modules First Prototypes, Proceeding of 11th International Conference on Concentrator Photovoltaic Systems-Aix Les Bains.



AIMS Press

© 2015 Luigi Mongibello, et al., licensee AIMS Press. This is an open access article distributed under the terms of the Creative Commons Attribution License (<http://creativecommons.org/licenses/by/4.0>)